

A mechanistic study on boron rejection by sea water reverse osmosis membranes

Hoon Hyung, Jae-Hong Kim*

School of Civil and Environmental Engineering, Georgia Institute of Technology, 200 Bobby Dodd Way, Atlanta, GA 30332, United States

Received 28 July 2006; received in revised form 14 September 2006; accepted 29 September 2006

Available online 5 October 2006

Abstract

Boron is a vital element for organism growth, but excessive exposure can cause detrimental effects to plants, animals, and possibly humans. However, it has been challenging for many of the existing sea water reverse osmosis (SWRO) membrane plants to remove boron and meet the current World Health Organization Guidelines for Drinking Water Quality. The objective of this study was to evaluate the effect of key operating parameters such as pH and temperature on boron rejection and develop a corresponding mechanistic predictive model. Bench-scale cross-flow filtration experiments were performed to estimate the rejection of boron by six commercial SWRO membranes. The rejection of boron appeared to follow a mechanism which is different from those of other ionic solutes and could not be readily correlated with their rejections. An irreversible thermodynamic model coupled with film theory was applied to quantitatively analyze the experimental observations. The model accurately predicted the boron rejection performances of the SWRO membranes at different operating conditions. The model was further modified to account for the boric acid speciation by pH and temperature dependence of the model parameters. The model developed herein will constitute fundamental for performance prediction and design of SWRO processes.

© 2006 Elsevier B.V. All rights reserved.

Keywords: Boron; Sea water; Reverse osmosis membrane; Model

1. Introduction

The sea water desalination is increasingly recognized as a viable alternative for potable water production due to localized scarcity and quality deterioration of fresh water sources. However, desalination practices have been challenged by increasingly stringent product water quality standards, as knowledge on the occurrence and subsequent environmental and human health impact of natural and anthropogenic compounds such as boron expands. Boron is naturally occurring and present in the sea water at an average concentration of 4.6 mg/L. It is an essential element for the growth of plants with the optimal concentration in water for agriculture purpose ranging from 0.3 to 0.5 mg/L [1]. However, if the concentration of boron is too high, massive leaf damages and/or premature ripening can occur, leading to reduced crop yields [2]. Toxicological effects of human exposure to excess boron, mostly reproductive and developmental, are

well documented [3]. Consequently, the World Health Organization (WHO) Guidelines for Drinking Water Quality suggested a maximum recommended boron concentration of 0.5 mg/L [4]. This value is, however, considered provisional due to the lack of a comprehensive toxicological assessment and limited availability of technologies to remove boron [4] and currently under reevaluation by the WHO.

The reverse osmosis (RO) process is one of the most widely used treatment options for sea water desalination. Despite its capacity to efficiently remove ionic species (typically over 99%), the RO process has not been very effective in boron removal. In general, the rejection of boron by RO membranes has been found to be lower than 90%, with rejection by some low-pressure brackish water RO (BWRO) membranes reaching as low as 40%. Even with specialized SWRO membranes that are designed for up to 95% boron rejection in the neutral pH condition, it is still difficult for a single-pass full-scale RO process to meet the current WHO boron guideline of 0.5 mg/L, while achieving required system recovery, unless additional treatment step is employed. For example, a pilot-scale single-pass SWRO plant operated at 40% recovery in Okinawa Island, Japan [5] produced

* Corresponding author. Tel.: +1 404 894 2216; fax: +1 404 385 7087.
E-mail address: jaehong.kim@ce.gatech.edu (J.-H. Kim).

permeates with 1.3 mg/L of boron. Boron rejections by eight RO desalination plants in Japan with varying design options were reported in the same study to range from 43% to 78% [5]. Other pilot and full-scale studies reported that a single-pass RO process with typical target recovery of 40–55% would produce the permeate with boron concentration ranging from 0.5 to 1.0 mg/L, which corresponded to overall boron removal by the system ranging from 80% and at most up to 90% [6,7]. As a result, it has been proposed that at least a double-pass RO configurations would be necessary in order to produce permeate boron concentration levels consistently below 1 mg/L [8]. Previous studies have also suggested that the boron rejection by the RO membrane would improve as pH increased, temperature decreased, and operating pressure increased [5,9–11].

In this study, boron rejections by six commercial SWRO membranes were evaluated using a bench-scale cross-flow filtration setup. The performance of each membrane was evaluated at different pH, temperature, and operating pressure conditions. A mathematical model was developed based on the irreversible thermodynamic model coupled with film theory to predict the effect of these operating conditions on the boron removal.

2. Theory

2.1. Mathematical model for solute rejection by RO membranes

According to the irreversible thermodynamic model (commonly referred to as the Kedem-Katchalsky or Spiegler-Kedem model) [12,13], transports of water and solute across an RO membrane are expressed as follows:

$$J_v = -p_h \left(\frac{dP}{dx} - \sigma \frac{d\pi}{dx} \right) \quad (1)$$

$$J_s = -p_s \frac{dC}{dx} + (1 - \sigma) J_v \bar{C} \quad (2)$$

where J_v is the volumetric water flux [LT^{-1}]; J_s is the gravimetric solute flux [$\text{ML}^{-2}\text{T}^{-1}$]; p_h is the specific hydraulic permeability coefficient [$\text{M}^{-1}\text{L}^3\text{T}$]; p_s is the local solute permeability coefficient [L^2T^{-1}]; P is the hydraulic pressure [$\text{ML}^{-1}\text{T}^{-2}$]; π is the osmotic pressure [$\text{ML}^{-1}\text{T}^{-2}$]; σ is the reflection coefficient; C is the superficial solute concentration [ML^{-3}] which is assumed to be in equilibrium with concentration of solute in the membrane phase; and \bar{C} is the average value of solute concentrations in the feed and permeate sides [ML^{-3}].

Eq. (1) implies that water permeation through an RO membrane is proportional to the difference between applied hydraulic pressure and osmotic pressure. The effect of the osmotic pressure is influenced by a reflection coefficient, which represents the extent of solute–water coupling. The reflection coefficient approaches unity for an ideal membrane and zero for a porous membrane (i.e., no osmotic pressure). Eq. (2) represents the solute transport through membrane. The first term in right hand side denotes the solute transport by diffusion which is proportional to a concentration gradient. The second term represents the solute transport by convection which is determined by the

degree of coupling between solutes and water, a solvent flux, and an average concentration of the solute between feed and permeate sides. When there is little or no coupling between the solutes and the solvents (i.e., $\sigma \approx 1$), the solute transport by convection becomes negligible.

The concentration of solutes near the membrane surface is different from that in the bulk phase due to concentration polarization, which results from the accumulation of solutes rejected by the membrane. The concentration at the membrane surface can be derived from the film theory and as follows [14]:

$$\frac{C_m - C_p}{C_f - C_p} = \exp\left(\frac{J_v}{k}\right) \quad (3)$$

where C_f is the feed concentration [ML^{-3}]; C_p is the permeate concentration [ML^{-3}]; C_m is the concentration at the membrane surface [ML^{-3}]; and k is the mass transfer coefficient [LT^{-1}]. Combining Eqs. (2) and (3), an apparent rejection (R_0) of the solutes by the membrane is expressed as follows:

$$\frac{R_0}{1 - R_0} = \frac{C_f - C_p}{C_p} = \frac{\sigma}{1 - \sigma} \cdot \frac{1 - \exp(-J_v \cdot (1 - \sigma)/P_s)}{\exp(-J_v/k)} \quad (4)$$

where $R_0 = (C_f - C_p)/C_f$ is the apparent rejection; $P_s = p_s/\Delta x$ is the overall permeability constant [LT^{-1}]; and Δx is the thickness of the separation layer [L].

2.2. Model parameter estimation

Unknown parameters such as mass transfer coefficient (k), solute overall permeability constant (P_s), and reflection coefficient (σ) in Eq. (4) were estimated as follows. First, the mass transfer coefficient of salt (NaCl) was determined using the following relationship [15]:

$$k_{\text{Salt}} = \frac{J_{v(\text{Salt})}}{\ln[(\Delta P/(\pi_{f(\text{Salt})} - \pi_{p(\text{Salt}))})(1 - (J_{v(\text{Salt})}/J_{v(\text{H}_2\text{O})})])]} \quad (5)$$

A filtration experiment was first performed with a salt solution and the volumetric permeate flux, $J_{v(\text{Salt})}$ [LT^{-1}], was measured. Osmotic pressures in the feed, $\pi_{f(\text{Salt})}$ [$\text{ML}^{-1}\text{T}^{-2}$], and the permeate, $\pi_{p(\text{Salt})}$ [$\text{ML}^{-1}\text{T}^{-2}$], were estimated by measuring respective salt concentrations and using an empirical relationship given below. Another filtration experiment was performed at the identical condition with pure water and $J_{v(\text{H}_2\text{O})}$ [LT^{-1}] was measured. Eq. (5) was derived based on the assumption that the reflection coefficient is very close to unity, which is valid for transport of most of ions through SWRO membranes. However, it might not be directly applicable to evaluate the mass transfer coefficient of boron, which generally shows less than 90% rejection by SWRO membranes (i.e., the reflection coefficient is less than unity). Since boron in a mass transfer boundary layer was under the same mixing condition as salts, the mass transfer coefficient of boron was estimated from the measured salt mass transfer coefficient using the following relationship [6,16]:

$$\frac{k_{\text{Salt}}}{k_B} = \left(\frac{D_{\text{Salt}}}{D_B} \right)^\beta \quad (6)$$

where D is the molecular diffusion coefficient [L^2T^{-1}] and β is the empirical coefficient = 2/3 for a clean membrane [17].

Once k was determined, σ and P_s could be obtained from a non-linear optimization of Eq. (4) using a set of experimentally measured apparent rejections (R_0) and water fluxes (J_v) of boron under varying pressures. The non-linear optimization was performed using a curve fitting tool box in MATLAB® (The Mathworks Inc., Natick, MA) with a trust region method, which proved to be successful in obtaining unique solutions (i.e., no local convergence).

2.3. Empirical equations for the sea water properties

Following empirical equations were used to estimate relevant properties of the synthetic sea water that are required for modeling [10,18]:

$$\pi(C_{\text{Salt}}, T) = (0.6955 + 0.0025 \times (T - 273.15)) \times 10^8 \frac{C_{\text{Salt}}}{\rho} \quad (7)$$

$$\rho = 498.4m + \sqrt{248400m^2 + 752.4m \times C_{\text{Salt}}} \quad (8)$$

(where $m = 1.0069 - 2.757 \times 10^{-4}(T - 273.15)$)

$$D_{\text{Salt}} = 6.725 \times 10^{-6} \exp\left(0.1546 \times 10^{-3} C_{\text{Salt}} - \frac{2513}{T}\right) \quad (9)$$

$$\mu = 1.234 \times 10^{-6} \exp\left(0.00212 C_{\text{Salt}} + \frac{1965}{T}\right) \quad (10)$$

where π is the osmotic pressure in Pa [$ML^{-1}T^{-2}$]; C_{Salt} is the concentration of salts in kg/m^3 [ML^{-3}]; T is the temperature in K; ρ is the density in kg/m^3 [ML^{-3}]; D_{Salt} is the diffusion coefficient of salt in m^2/s [L^2T^{-1}]; and μ is the viscosity in Pa s [$ML^{-1}T^{-1}$].

3. Experimental

3.1. Materials

Six commercial polyamide thin-film composite SWRO membranes obtained from four representative membrane manufacturers were used in this study. Salt rejections and permeate fluxes of these membranes ranged from 99.6% to 99.8% and 25.5 to 38.3 L/m² h (15–22.5 gal/ft² day), respectively, based on specifications provided by the manufacturers. Detailed specifications of these membranes and test conditions are summarized in Table 1.

Table 1
Specification of the SWRO membranes

| Manufacturer | Saehan | Hydranautics | Dow (filmtec) | Dow (filmtec) | Toray | Toray |
|--|---------------------|---------------------|---------------------|---------------------|---------------------|---------------------|
| Model | SR | SWC4+ | SW30 HR XLE | SW30 HR LE | TM820 | TM820A |
| Material | Polyamide composite |
| Rejection ^a (%) | 99.6 | 99.8 | 99.7 | 99.75 | 99.75 | 99.75 |
| Flux ^{a,b} (L/m ² h) | 26.9 | 29.1 | 38.3 | 32.0 | 28.1 | 25.5 |

^a Test condition: 25 °C, 55.16 × 10⁵ Pa (800 psi), 32,000 mg/L NaCl feed solution, 8% recovery.

^b Calculated based on permeate flow rates and membrane module areas provided by the manufacturers.

rized in Table 1. All the filtration experiments were performed using a synthetic solution containing 10,500 mg/L sodium, 19,000 mg/L chloride, 1350 mg/L magnesium, 450 mg/L calcium, and 2700 mg/L sulfate (i.e., total dissolved solids of 34,000 mg/L) which represented the average inorganic composition of sea water [19]. Boric acid was spiked in the feed water at 5 mg/L as boron.

3.2. Experimental setup

The bench-scale membrane test unit was designed to test four membranes at the same time and composed of two parallel feed lines with each line accommodating two plate and frame membrane test cells in series. A feed channel in each test cell was rectangular shape, 73 mm in length and 38 mm in width to provide an effective filtration area of 2.774 × 10⁻³ m² with feed flow channel height of 5 mm and experiments were performed without a feed spacer. Each cell had upper and lower stainless steel (SS)-316 plates and a flat sheet membrane, which was sealed with a silicon rubber ring, was sandwiched in between. Feed water stored in a 21.8 L tank was circulated and pressurized by a positive displacement high pressure pump (Hydra-Cell D10S, Wanner Engineering, Minneapolis, MN), which could deliver 30.3 L/min (8.0 gal/min) (GPM) of water at up to 6.9 × 10⁶ Pa (1000 psi) of discharge pressure. Since both the concentrate and the permeate were returned to the feed tank and the volume of permeate samples was less than 0.1% of total feed volume, feed concentration was maintained constant. Feed temperature was regulated by a temperature controller (Polystat, Cole parmer, Vernon Hills, IL) by circulating cooling water through a heat exchange coil immersed inside of the feed tank. System pressure was controlled with a needle valve (Swagelok, Solon, OH) and monitored with a pressure gauge (Swagelok, Solon, OH) located downstream of the cells. To prevent the overpressurization of the system, a safety valve (C22AB, Wanner Engineering, Minneapolis, MN) was installed next to the pump outlet. The feed flow rate was measured by a hydraulic flow meter (King, Atlanta, GA) and the permeate flow rate was measured using a HFM 1000 digital flow meter (Agilent, Palo Alto, CA). All experimental components were made of SS-316 and/or Teflon® to avoid corrosion.

3.3. Experimental procedure

For quality control purpose, the salt rejection and the flux of each membranes at standard test condition of the manufacturer were measured after an initial stabilization stage (i.e., membrane pressurization at 6.9 × 10⁶ Pa (1000 psi) for 48 h)

and the experiment proceeded only when the salt rejection and the flux of the membrane were within 0.5% and 10%, respectively, of those specified by the manufacturer. Two sets of experiments were performed for each membrane to investigate the effect of pH and temperature on boron rejection. The pH effect experiment was performed at four different pHs of 6.2, 7.5, 8.5, and 9.5 at constant temperature of 25 °C. Temperature effect experiment was performed at three different temperatures of 15, 25, and 35 °C at two pH conditions of 6.2 and 9.5. For each pH and temperature condition, trans-membrane pressure was varied from 41.4×10^5 to 6.9×10^6 Pa (600 to 1000 psi) by 6.9×10^6 Pa (100 psi) increment. The pH of solution was adjusted by adding NaOH or HCl while monitoring pH using a Thermo Orion 230 + pH meter (Waltham, MA). The cross-flow velocity was maintained at 0.17 m/s during all the experiments. To prevent leaching of boron from glassware, only polyethylene sample bottles were used for sample delivery.

3.4. Analytical methods

Surface potentials of the membrane were analyzed by an electrophoretic method [20] using an ELS8000 electrophoretic light scattering analyzer (Otsuca, Osaka, Japan). Ionic strength of the test solution was maintained at 0.005 using NaCl and pH was controlled at between 4 and 10 by adding HCl or NaOH. Concentrations of boron, sodium, calcium, and magnesium were measured according to EPA method 200.7 [21] using an inductively coupled plasma-atomic emission spectroscopy (ICP-AES) (Model ICAP 61E Trace Analyzer, Thermo Jarrell Ash, Franklin, MA). Measurements were performed six times for each sample and the average value was reported. Concentrations of chloride and sulfate ions were measured following EPA method 300.1 [22] using a Dionex DX-600 ion chromatography (IC) system (Sunnyvale, CA), which was equipped with an IonPac AG9 HC guard column, an IonPac AS9 HC analytical column (4 mm \times 250 mm), and an ED50 conductivity detector and 9.0 mM sodium carbonate solution was used as an eluent. Standard solutions for ICP-AES and IC calibrations were prepared using the High-Purity Standards (Charleston, SC) solutions.

4. Results and discussions

4.1. Effect of pH on boron rejection

Boron rejection was largely dependent on pH and increased as pH increased, consistent with the previous studies [6,7,11], while the rejections of other ionic species were not. The boron rejections by all the six membranes at varying pHs and pressures were plotted against the rejections of a representative ionic species (chloride ion) in Fig. 1a. Alternatively, the boron rejections by one representative membrane (Saehan SR) at varying pHs and pressures were plotted versus rejections of all the ionic species (i.e., chloride, sulfate, sodium, calcium, and magnesium) in Fig. 1b. The data in the figures were scattering, making it difficult to find any meaningful correlation between boron rejection

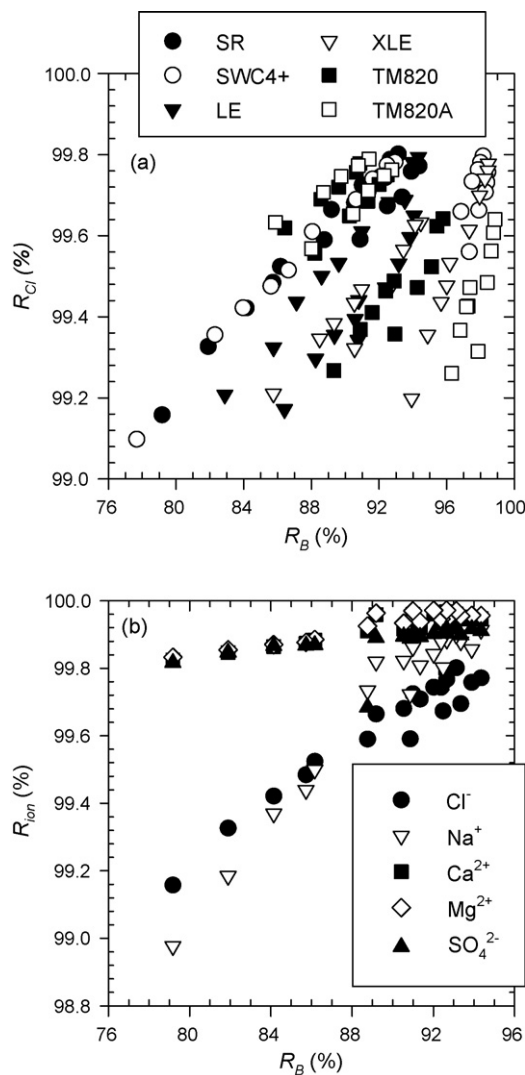


Fig. 1. (a) Boron rejection vs. chloride ion rejection for all the membranes tested and (b) boron rejection vs. rejections of ionic species for the Saehan SR membrane.

and ionic species rejection. Only portions of data in Fig. 1a and b that obtained from the experiments performed at the same pH with different pressures showed an apparent linear relationship, which was consistent with the suggestion by [6] that salt rejection showed a linear correlation with boron rejection at unaltered pH condition. However, when the pH effect was taken into consideration, the rejection of other ionic species would not be indicative of boron rejection.

Experimental data obtained with varying pressures at each pH were fitted to Eq. (4) along with corresponding mass transfer coefficients obtained from independent experiments. Estimated transport parameters are presented in Table 2. Model curves plotted using the parameters are compared with experimental data in Fig. 2. The parameter estimation method used in this study appeared accurate, as most of the correlation coefficients (r^2) calculated from five observation per each curve were higher than 0.98 (Table 2). Mass transfer coefficients of boron (k_B) had little pH dependency but permeability constants of boron (P_{sB}) decreased and reflection coefficients of boron (σ_B)

Table 2
Result of the parameter estimation for the pH effect experiment

| Membranes | pH | k_B (cm/s) | P_{SB} (cm/s) | σ_B | r^2 |
|-----------|-----|--------------|-----------------|------------|-------|
| SR | 6.2 | 1.84E-03 | 5.47E-05 | 0.975 | 0.988 |
| | 7.5 | 1.68E-03 | 6.11E-05 | 0.994 | 0.987 |
| | 8.5 | 2.03E-03 | 4.65E-05 | 0.991 | 0.995 |
| | 9.5 | 1.78E-03 | 1.40E-05 | 0.993 | 0.933 |
| SWC4+ | 6.2 | 2.38E-03 | 3.84E-05 | 0.983 | 0.995 |
| | 7.5 | 2.36E-03 | 3.92E-05 | 0.992 | 0.997 |
| | 8.5 | 2.86E-03 | 2.84E-05 | 0.986 | 0.996 |
| | 9.5 | 2.74E-03 | 7.24E-06 | 0.996 | 0.970 |
| XLE | 6.2 | 2.65E-03 | 4.15E-05 | 0.962 | 0.992 |
| | 7.5 | 2.62E-03 | 4.21E-05 | 0.970 | 0.995 |
| | 8.5 | 2.69E-03 | 3.24E-05 | 0.977 | 0.993 |
| | 9.5 | 2.42E-03 | 9.48E-06 | 0.988 | 0.984 |
| LE | 6.2 | 2.07E-03 | 3.33E-05 | 0.982 | 0.992 |
| | 7.5 | 2.08E-03 | 3.61E-05 | 0.993 | 0.994 |
| | 8.5 | 2.44E-03 | 2.51E-05 | 0.988 | 0.987 |
| | 9.5 | 2.38E-03 | 6.82E-06 | 0.998 | 0.977 |
| TM820 | 6.2 | 1.82E-03 | 4.36E-05 | 0.981 | 0.985 |
| | 7.5 | 1.80E-03 | 4.74E-05 | 0.999 | 0.997 |
| | 8.5 | 2.17E-03 | 3.40E-05 | 0.994 | 0.996 |
| | 9.5 | 2.05E-03 | 8.93E-06 | 0.999 | 0.994 |
| TM820A | 6.2 | 2.50E-03 | 2.76E-05 | 0.982 | 0.990 |
| | 7.5 | 2.50E-03 | 2.85E-05 | 0.991 | 0.992 |
| | 8.5 | 3.07E-03 | 2.11E-05 | 0.993 | 0.985 |
| | 9.5 | 2.85E-03 | 6.07E-06 | 0.999 | 0.992 |

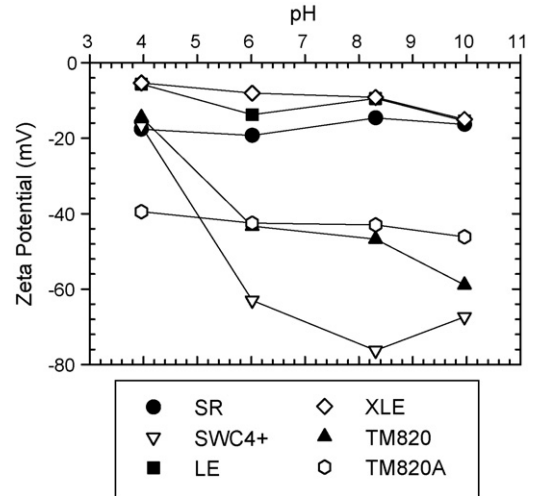
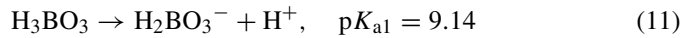


Fig. 3. Surface charges of the SWRO membranes at different pHs (at $I=0.005$).

increased as pH increased. Combined effect of P_{SB} decrease and σ_B increase resulted in increased boron rejections (i.e., increase in $R_0/(1 - R_0)$ in Fig. 2) at higher pHs.

The observed pH dependence of P_{SB} and σ_B resulted since boron exists as boric acid (H_3BO_3) and deprotonated borate ion ($H_2BO_3^-$) with the corresponding first acid dissociation constant (pK_{a1}) of 9.14 at 25 °C in a low ionic strength solution

[8,11,23]. Complexation of boric acid and borate ion with other metal ions is negligible [23,24]. At a natural pH range, a majority of boron exists as uncharged boric acid. However, the fraction of negatively-charged borate ion increases as pH increases and borate ion becomes a dominant species as pH increases beyond pK_{a1} :



This acid–base speciation change is of particular importance since the surfaces of all the membranes tested are negatively charged for the pH range investigated (Fig. 3). Consequently, as pH increases, the charge repulsion between negatively charged borate ion and the negatively charged membrane surface plays a more important role on the overall rejection of boron. Specifically, increased charge repulsion at higher pH resulted in decreased diffusive transport of boron through the membrane

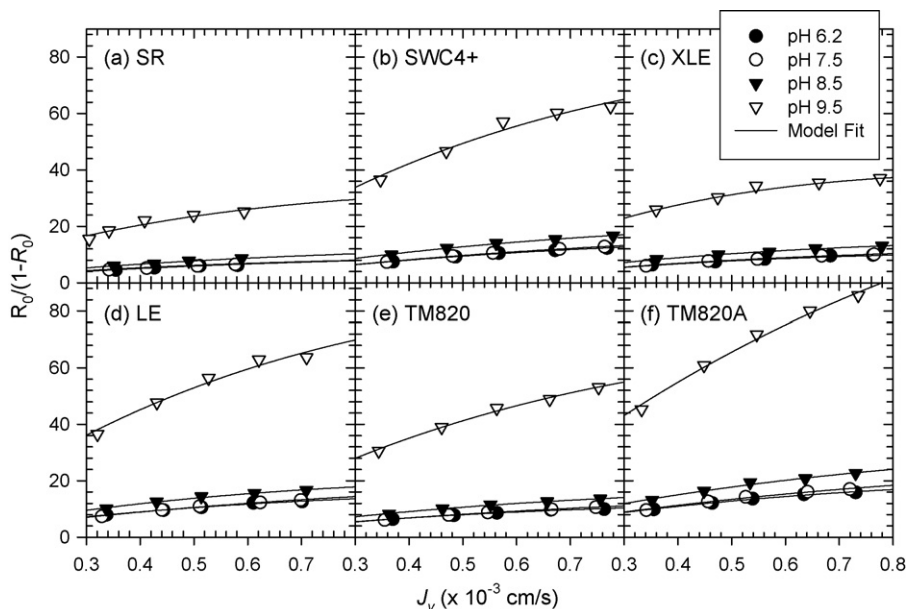


Fig. 2. Boron rejection at varying pHs and 25 °C and corresponding model fit. Different data points for each pH were obtained under varying transmembrane pressures 41.4×10^5 – 6.9×10^6 Pa (600–1000 psi).

(decreased P_{sB}) and reduced solute–solvent coupling (increased σ_B).

The observed pH dependence was quantitatively analyzed by considering that the overall transport of boron was the sum of individual and independent contributions from boric acid and borate ion. Consequently, the following equation was developed to predict the permeability constant of boron:

$$P_{sB} = \alpha_0 \times P_{s(H_3BO_3)} + \alpha_1 \times P_{s(H_2BO_3^-)} \quad (12)$$

where $P_{s(H_3BO_3)}$ is the permeability constant of boric acid [LT^{-1}] and $P_{s(H_2BO_3^-)}$ is the permeability constant of borate ion [LT^{-1}]. A similar predictive approach was applied to estimate the reflection coefficient of boron at any pH:

$$\sigma_B = \alpha_0 \times \sigma_{(H_3BO_3)} + \alpha_1 \times \sigma_{(H_2BO_3^-)} \quad (13)$$

where $\sigma_{(H_3BO_3)}$ is the reflection coefficient of boric acid and $\sigma_{(H_2BO_3^-)}$ is the reflection coefficient of borate ion. In the above equations, α_0 and α_1 represent the fraction of boric acid and borate ion, respectively. Since ionic strength of the feed solution was extremely high, following definitions for α_0 and α_1 were used [24]:

$$\alpha_0 = \frac{\{H^+\}}{\{H^+\} + K'_{a1}} = \frac{[H_3BO_3]}{C_B} \quad (14)$$

$$\alpha_1 = \frac{K'_{a1}}{\{H^+\} + K'_{a1}} = \frac{[H_2BO_3^-]}{C_B} = 1 - \alpha_0 \quad (15)$$

$$K'_{a1} = \frac{[H_2BO_3^-]\{H^+\}}{[H_3BO_3]} \quad (16)$$

where $[H_3BO_3]$ is the concentration of boric acid [ML^{-3}]; $[H_2BO_3^-]$ is the concentration of borate ion [ML^{-3}]; $\{H^+\}$ is the activity of proton [ML^{-3}]; and K'_{a1} is the apparent first acid dissociation constant for boric acid [ML^{-3}]. Note that K'_{a1} is defined using the concentrations of boron species and the activity of proton, both of which are readily measurable parameters. The value of K'_{a1} depends on salinity and temperature according

Table 3

Permeability constants and reflection coefficients of boric acid and borate ion from the pH effect experiment

| Membranes | $P_{s(H_3BO_3)}$ (cm/s) | $P_{s(H_2BO_3^-)}$ (cm/s) | $\sigma_{(H_3BO_3)}$ | $\sigma_{(H_2BO_3^-)}$ |
|-----------|-------------------------|---------------------------|----------------------|------------------------|
| SR | 5.47E-05 | 8.76E-06 | 0.975 | 0.996 |
| SWC4+ | 3.84E-05 | 3.13E-06 | 0.983 | 0.997 |
| XLE | 4.15E-05 | 5.26E-06 | 0.962 | 0.991 |
| LE | 3.33E-05 | 3.41E-06 | 0.982 | 1.000 |
| TM820 | 4.36E-05 | 4.66E-06 | 0.981 | 1.000 |
| TM820A | 2.76E-05 | 3.23E-06 | 0.981 | 1.000 |

to the following empirical equation [25]:

$$-\log K'_{a1} = \frac{2291.9}{T} + 0.01756 - 3.385 - 3.904 \times S^{1/3} \quad (17)$$

where T is the temperature in K and S is the total salt concentration (salinity) in ppm [ML^{-3}]. At a representative sea water salinity of 34,000 ppm and 25 °C, pK'_{a1} is estimated at 8.68, which is much lower than 9.14 in a dilute solution. Note that the salinity near the membrane surface further increases due to concentration polarization. Moreover, the salt concentration in a concentration polarization layer would depend on membranes due to differences in rejection performances of the membranes. Therefore, K'_{a1} for each membrane and pH condition was individually calculated from Eq. (17) using a wall concentration (C_m) of salt estimated from Eq. (3) and found to range from 8.59 to 8.63.

Permeability constants of boric acid ($P_{s(H_3BO_3)}$) and borate ion ($P_{s(H_2BO_3^-)}$) for each membrane were calculated by substituting known parameters (P_{sB} , α_0 , and α_1) at pH 6.2 and 9.5 into Eq. (12), respectively, and solving the resulting set of equations. Results summarized in Table 3 suggested that $P_{s(H_3BO_3)}$ was approximately six to twelve times higher than $P_{s(H_2BO_3^-)}$ for the membranes investigated. Once $P_{s(H_3BO_3)}$ and $P_{s(H_2BO_3^-)}$ were determined, the overall permeability constant of boron (P_{sB}) at any pH could be estimated using Eq. (12) as shown in Fig. 4.

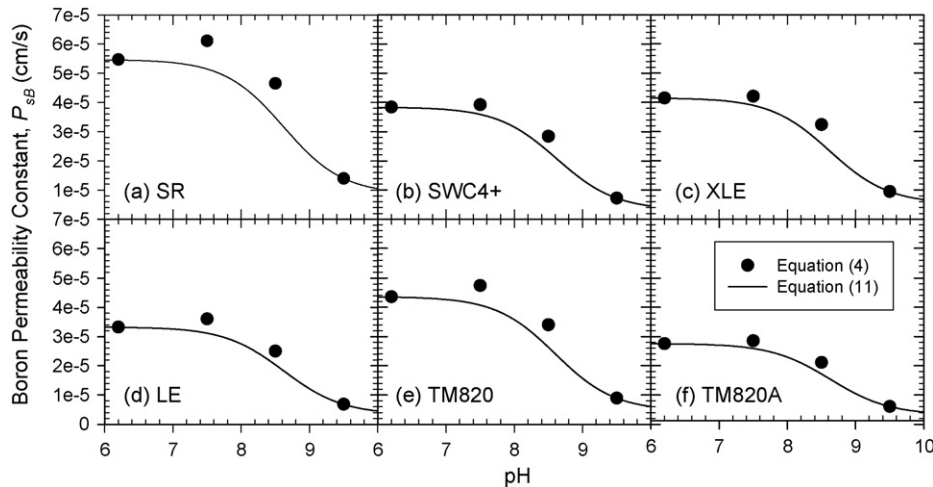


Fig. 4. Effect of pH on boron permeability constant (P_{sB}). The symbols were determined from fitting Eq. (4) to the experimental data. Lines represent the result of fitting the observed pH dependence with Eq. (11).

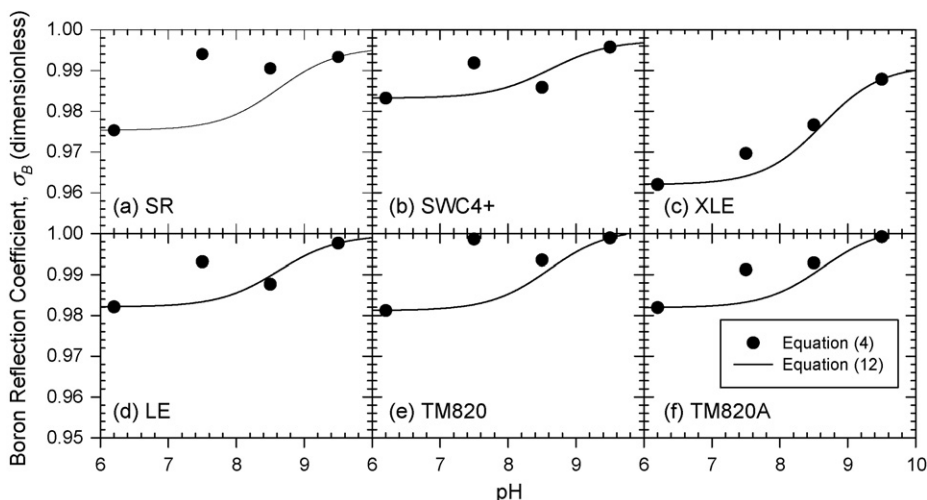


Fig. 5. Effect of pH on boron reflection constant (σ_B). The symbols were determined from fitting Eq. (4) to the experimental data. Lines represent the result of fitting the observed pH dependence with Eq. (12).

Reflection coefficients of boric acid ($\sigma_{(H_3BO_3)}$) and borate ion ($\sigma_{(H_2BO_3^-)}$) were calculated using Eq. (13) following the same approach used above and the results are presented in Table 3. $\sigma_{(H_3BO_3)}$ ranged from 0.962 to 0.983 depending on membrane and it mostly accounted for low σ_B values. In contrast, $\sigma_{(H_2BO_3^-)}$ was very close to unity regardless of the membrane type. This suggested that solvent coupling was negligible for borate ion and the borate ion permeation mostly depended on the diffusive transport. In other words, all the membranes could effectively reject borate ions in a similar manner with other anionic species such as chloride and sulfate. Fig. 5 compares the reflection coefficients of boron (σ_B) predicted from Eq. (13) to those determined from the experiments and Eq. (4). Some deviations were most likely due to relatively small changes in σ_B . Note that since the overall transport of boron is dependent more on the diffusive

transport, small variations in the solvent coupling would have a negligible effect on the overall estimation of boron transport using Eq. (4).

4.2. Effect of temperature on boron rejection

Experimental results obtained from the temperature effect experiments at two pH conditions (6.2 and 9.5) for four membranes (SWC4+, LE, TM820, and TM820A) are shown in Fig. 6. Each data set at fixed pH and temperature with varying pressures was fitted with Eq. (4) using the non-linear optimization method and mass transfer coefficient independently evaluated. The model prediction using the fitted parameters matched the experimental data very accurately (Fig. 6). For all the membranes at both pHs, the rejection of boron decreased

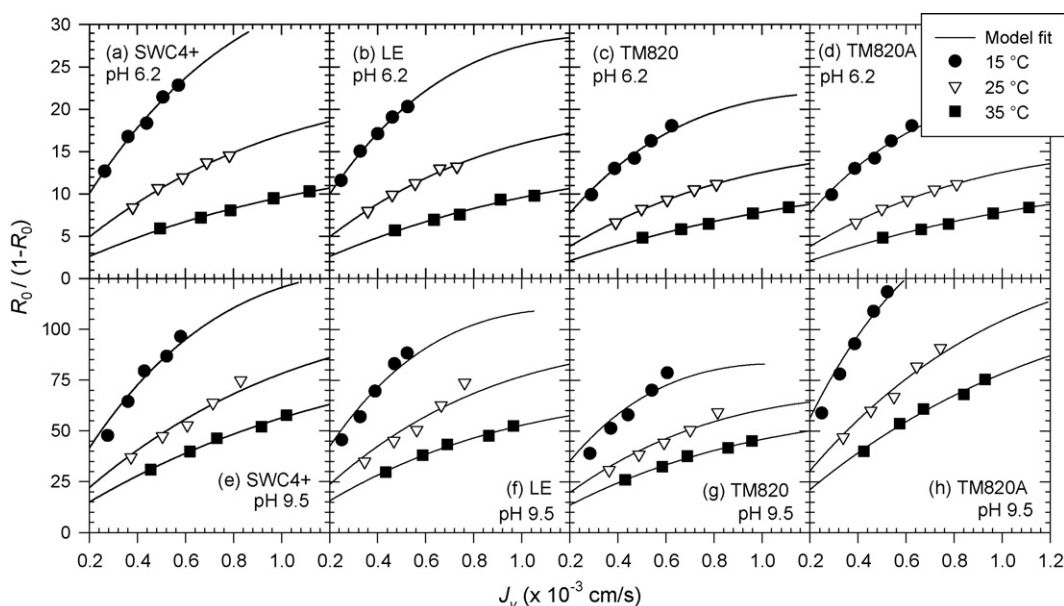


Fig. 6. Boron rejection at varying temperatures and two pHs (6.2 and 9.5) and corresponding model fit. Different data points for each temperature were obtained under varying transmembrane pressures 41.4×10^5 – 6.9×10^6 Pa (600–1000 psi).

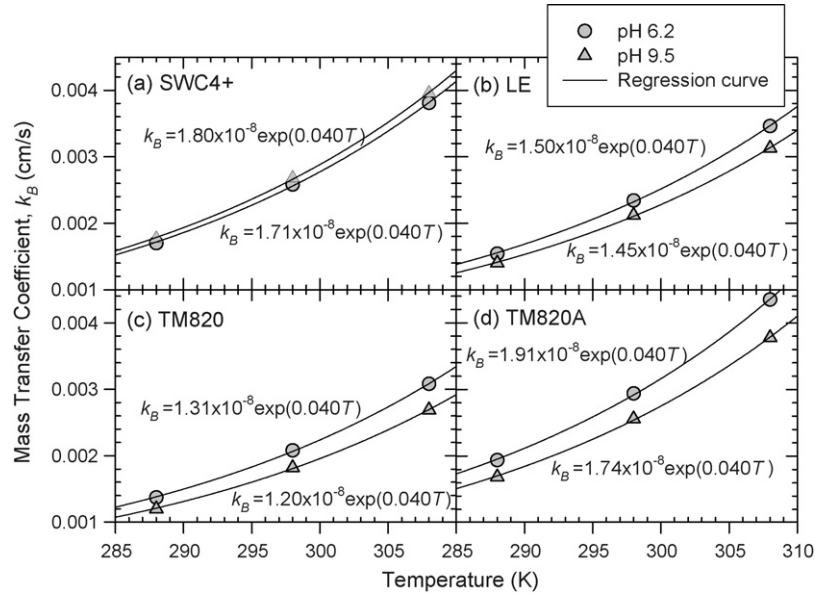


Fig. 7. Effect of temperature on boron mass transfer coefficient in concentration polarization layer (k_B). The symbols were determined from fitting Eq. (4) to the experimental data. Lines represent the result of fitting the observed temperature dependence with Eq. (17).

(i.e., $R_0/(1-R_0)$ decreased) as temperature increased. Note that both the specific hydraulic permeability (p_h) in Eq. (1) and the local solute permeability (p_s) in Eq. (2) would increase as temperature increases. Therefore, the temperature dependence of solute rejection would be determined by a trade-off between temperature dependence of p_s and that of p_h (i.e., evidenced by approximately 70–90% increase in the permeate flux for the membrane tested when temperature increased from 15 to 35 °C). The experimental result implies that the temperature dependence of p_s overwhelms that of p_h .

Temperature dependence of the transport parameters was further analyzed using an empirical equation by [26] where both solute mass transfer coefficient across the boundary layer (k) and solute transport parameter ($D_{AM}K/\Delta x$) were assumed to be exponential functions of temperature as follows:

$$k \text{ or } \left(\frac{D_{AM}K}{\Delta x} \right) \propto \exp(\text{constant} \times T) \quad (18)$$

where D_{AM} is the diffusion coefficient of solute in the membrane [L^2T^{-1}]; K is the partition coefficient of solute between water and membrane; and Δx is the thickness of membrane [L]. The pre-exponent constant was determined to be 0.005, for example, for a cellulose acetate membrane filtering salt solution [26]. The same general equation was applied to express the temperature dependence of mass transfer coefficient as well as permeability constants and reflection coefficients of both boric acid and borate ion.

Experimentally determined mass transfer coefficients are plotted against temperature in Fig. 7 along with non-linear regression curve-fits using Eq. (18). Increase in k_B with temperature accurately followed the exponential function with pre-exponent constant of 0.04 for all membranes and pHs investigated.

$P_{s(H_3BO_3)}$, $P_{s(H_2BO_3^-)}$, $\sigma_{(H_3BO_3)}$, and $\sigma_{(H_2BO_3^-)}$ at 15, 25, and 35 °C were individually evaluated following the same method

used for pH effect data analysis. Briefly, salt concentration at the membrane wall (C_m) was estimated from Eq. (3) using the mass transfer coefficients and experimental data (C_f , C_p , and J_v). From the obtained C_m , the apparent acid constant of boric acid (K'_{a1}) was calculated using Eq. (17). The fractions of boric acid (α_0) and borate ion (α_1) were estimated from Eqs. (14) and (15) using K'_{a1} 's. Finally, $P_{s(H_3BO_3)}$ and $P_{s(H_2BO_3^-)}$ at each temperature were estimated by substituting the obtained parameters (P_{sB} , α_0 , and α_1) at pH 6.2 and 9.5 into Eq. (12), respectively, and solving the resulting sets of equations. $\sigma_{(H_3BO_3)}$ and $\sigma_{(H_2BO_3^-)}$ at each temperature were obtained from Eq. (13) following the same approach.

Obtained $P_{s(H_3BO_3)}$ and $P_{s(H_2BO_3^-)}$ were plotted versus temperature and fitted to Eq. (18) in Fig. 8. Pre-exponent constants were within a fairly narrow range of 0.066–0.068 for $P_{s(H_3BO_3)}$ and 0.048–0.049 for $P_{s(H_2BO_3^-)}$. Therefore, it again appeared that a single pre-exponent constant might be able to describe the temperature dependence of boron permeability for the membranes investigated. In contrast, the temperature dependence of $\sigma_{(H_3BO_3)}$ and $\sigma_{(H_2BO_3^-)}$ appeared to be negligible, as these parameters for all the membranes did not much changed by temperature.

Consequently, the temperature dependence of boron transport parameters can be summarized in the following equations:

$$k_{BT} = k_{B0} \exp(0.040(T - T_0)) \quad (19)$$

$$P_{s(H_3BO_3)T} = P_{s(H_3BO_3)0} \exp(0.067(T - T_0)) \quad (20)$$

$$P_{s(H_2BO_3^-)T} = P_{s(H_2BO_3^-)0} \exp(0.049(T - T_0)) \quad (21)$$

where k_{BT} is the mass transfer coefficient of boron at temperature T (K) [LT^{-1}]; k_{B0} is the mass transfer coefficient of boron at temperature T_0 [LT^{-1}]; $P_{s(H_2BO_3^-)T}$ is the permeability constant of boric acid at temperature T [LT^{-1}]; $P_{s(H_3BO_3)0}$ is the permeability constant of boric acid at temperature T_0 [LT^{-1}];

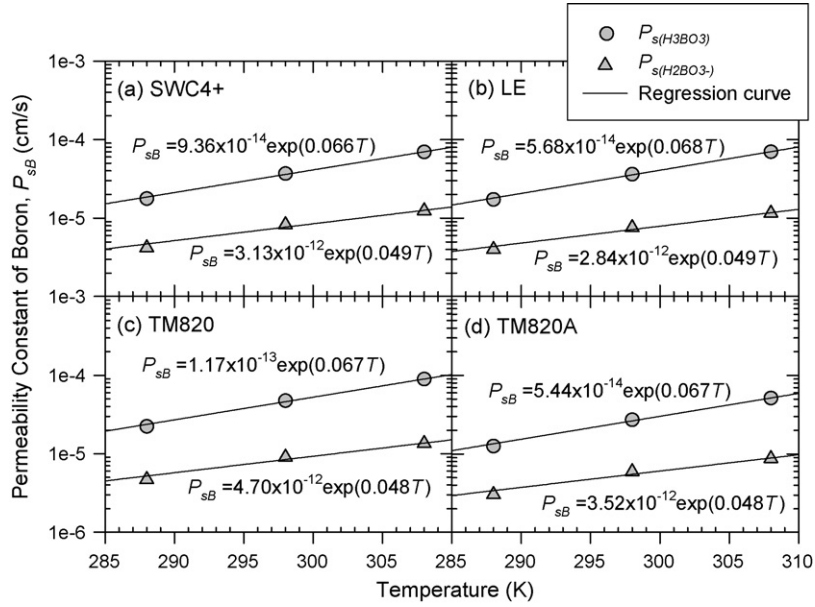


Fig. 8. Effect of temperature on boron permeability constant (P_{sB}). The symbols were determined from fitting Eq. (4) to the experimental data. Lines represent the result of fitting the observed temperature dependence with Eq. (17).

$P_{s(H_2BO_3^-)_T}$ is the permeability constant of borate ion at temperature T [LT^{-1}]; and $P_{s(H_2BO_3^-)_0}$ is the permeability constant of borate ion at temperature T_0 [LT^{-1}].

5. Conclusion

Bench-scale experiments performed with six commercial RO membranes under diverse operating conditions suggested that boron rejection was largely influenced by pH due to dissociation of weak boric acid. Operating temperature and pressure also affected boron rejection. The experimental results were quantitatively analyzed using the irreversible thermodynamic model coupled with film theory. The model was modified to account for the effect of pH and temperature on the overall boron transport as well as the effect of ionic strength on acid–base species equilibrium. In summary, key transport parameters that characterize boron transport over the range of condition investigated can be expressed using the following equations developed in this study:

$$k_{BT} = k_{B0} \exp(0.040(T - T_0)) \quad (19)$$

$$P_{sB} = \frac{\{H^+\}}{\{H^+\} + K'_{al}} \times P_{s(H_3BO_3)_0} \exp(0.067(T - T_0)) + \frac{K'_{al}}{\{H^+\} + K'_{al}} \times P_{s(H_2BO_3^-)_0} \exp(0.049(T - T_0)) \quad (22)$$

$$\sigma_B = \frac{\{H^+\}}{\{H^+\} + K'_{al}} \times \sigma_{(H_3BO_3)_0} + \frac{K'_{al}}{\{H^+\} + K'_{al}} \times \sigma_{(H_2BO_3^-)_0} \quad (23)$$

From this set of equations, the changes in the boron transport parameters as a function of pH ($-\log\{H^+\}$) and temperature can be predicted. Note that the pH dependence of k_B and

the temperature dependence of σ_B were negligible. These equations will provide basis for the prediction of boron removal performance by full-scale SWRO processes when combined with a model addressing non-homogeneous condition inside a membrane module (i.e., for example, [27]).

Acknowledgements

This research was supported by the Desalination and Water Purification Research and Development Program, Bureau of Reclamation, US Department of Interior (Agreement No. 04-FC-81-050, Project Manager: Frank Leitz). The authors would like to acknowledge Saehan Industries Inc., Hydranautics, Dow (Filmtec) Corporation, and Toray America for their donation of SWRO membranes. The authors also thank Noeon Park and Dr. Jaeweon Cho at Gwangju Institute of Science and Technology, Korea for the help with membrane surface analysis.

Nomenclature

| | |
|-----------|---|
| C | superficial solute concentration [ML^{-3}] |
| \bar{C} | average solute concentration of feed and permeate sides [ML^{-3}] |
| D | molecular diffusion coefficient [L^2T^{-1}] |
| J_s | gravimetric solute flux [$ML^{-2}T^{-1}$] |
| J_v | volumetric water flux [LT^{-1}] |
| k | mass transfer coefficient [LT^{-1}] |
| K | partition coefficient between solvent (water) and membrane |
| K'_{al} | apparent first acid constant of boric acid [ML^{-3}] |
| p_h | specific hydraulic permeability [$M^{-1}L^3T$] |
| p_s | local solute permeability coefficient [L^2T^{-1}] |

| | |
|------------|--|
| P | hydraulic pressure [$\text{ML}^{-1}\text{T}^{-2}$] |
| P_s | overall permeability constant [LT^{-1}] |
| R_0 | apparent rejection |
| T | temperature |
| Δx | thickness of a separation layer [L] |

Greek letters

| | |
|------------|--|
| α_0 | fraction of boric acid |
| α_1 | fraction of borate ion |
| μ | viscosity [$\text{ML}^{-1}\text{T}^{-1}$] |
| π | osmotic pressure [$\text{ML}^{-1}\text{T}^{-2}$] |
| σ | reflection coefficient |
| ρ | density [ML^{-3}] |

Subscripts

| | |
|-------------------------------|-------------------|
| B | boron |
| f | feed |
| (H_3BO_3) | boric acid |
| (H_2BO_3^-) | borate ion |
| (H_2O) | pure water |
| m | membrane surface |
| p | permeate |
| Salt | salt |
| T | temperature T |
| 0 | temperature T_0 |

References

- [1] N. Nadav, Boron removal from seawater reverse osmosis permeate utilizing selective ion exchange resin, *Desalination* 124 (1999) 131–135.
- [2] USEPA, Preliminary Investigation of Effects on the Environment of Boron, Indium, Nickel, Tin, Vanadium, and Their Compounds, EPA 56/2-75-005A, 1975.
- [3] USEPA, Toxicological Review of Boron and Compounds, EPA 635/04/052, 2004.
- [4] WHO, Addendum to Guidelines for Drinking Water Quality, second ed., vol. 2, Geneva, 1998.
- [5] Y. Magara, T. Aizawa, S. Kunikane, M. Itoh, M. Kohki, M. Kawasaki, H. Takeuti, The behavior of inorganic constituents and disinfection by products in reverse osmosis water desalination process, *Water Sci. Technol.* 34 (1996) 141–148.
- [6] M. Taniguchi, M. Kurihara, S. Kimura, Boron reduction performance of reverse osmosis seawater desalination process, *J. Membr. Sci.* 183 (2001) 259–267.
- [7] J. Redondo, M. Busch, J.P. De Witte, Boron removal from seawater using filmtec (Tm) high rejection SWRO membranes, *Desalination* 156 (2003) 229–238.
- [8] Y. Magara, A. Tabata, M. Kohki, M. Kawasaki, M. Hirose, Development of boron reduction system for sea water desalination, *Desalination* 118 (1998) 25–33.
- [9] P. Glueckstern, M. Priel, Optimization of boron removal in old and new SWRO systems, *Desalination* 156 (2003) 219–228.
- [10] A. Sagiv, R. Semiat, Analysis of parameters affecting boron permeation through reverse osmosis membranes, *J. Membr. Sci.* 243 (2004) 79–87.
- [11] D. Prats, M.F. Chillon-Arias, M. Rodriguez-Pastor, Analysis of the influence of pH and pressure on the elimination of boron in reverse osmosis, *Desalination* 128 (2000) 269–273.
- [12] O. Kedem, A. Katchalsky, Physical interpretation of phenomenological coefficients of membrane permeability, *J. Gen. Physiol.* 45 (1961) 143–179.
- [13] K.S. Spiegler, O. Kedem, Thermodynamics of hyperfiltration (reverse osmosis): criteria for efficient membranes, *Desalination* 1 (1966) 311–326.
- [14] E.L. Cussler, *Diffusion*, Cambridge University Press, Cambridge, 1984.
- [15] I. Sutzkover, D. Hasson, R. Semiat, Simple technique for measuring the concentration polarization level in a reverse osmosis system, *Desalination* 131 (2000) 117–127.
- [16] Y. Winograd, A. Solan, M. Toren, Mass-transfer in narrow channels in presence of turbulence promoters, *Desalination* 13 (1973) 171–186.
- [17] R.I. Urama, B.J. Mariñas, Mechanistic interpretation of solute permeation through a fully aromatic polyamide reverse osmosis membrane, *J. Membr. Sci.* 123 (1997) 267–280.
- [18] M. Taniguchi, S. Kimura, Estimation of transport parameters of RO membranes for Seawater Desalination, *AIChE J.* 46 (2000) 1967–1973.
- [19] V.L. Snoeyink, D. Jenkins, *Water Chemistry*, John Wiley & Sons, New York, 1980.
- [20] B. Kwon, S. Lee, J. Cho, H. Ahn, D.H.S. Lee, Shin, biodegradability, DBP formation, and membrane fouling potential of natural organic matter: characterization and controllability, *Environ. Sci. Technol.* 39 (2005) 732–739.
- [21] USEPA, Method 200.7, Trace Elements in Water, Solids, and Biosolids by Inductively Coupled Plasma-Atomic Emission Spectrometry, EPA-821-R-01-010, Washington, D.C., 2001.
- [22] USEPA, Method 300.1, Determination of Inorganic Anions in Drinking Water by Ion Chromatography, EPA 300.1-1, Cincinnati, 1999.
- [23] W. Stumm, J.J. Morgan, *Aquatic Chemistry*, third ed., Wiley-Interscience, New York, 1996.
- [24] J.P. Riley, G. Skirrow, *Chemical Oceanography*, vol. 2, second ed., Academic, New York, 1975.
- [25] J.M. Gieskes, in: E.D. Goldberg (Ed.), *The Sea*, vol. 5, Wiley-Interscience, New York, 1974.
- [26] S. Sourirajan, *Reverse Osmosis*, Logos Press Ltd., London, 1970.
- [27] B. Mi, C.L. Eaton, J.H. Kim, C.K. Colvin, J.C. Lozier, B.J. Mariñas, Removal of biological and non-biological viral surrogates by spiral-wound reverse osmosis membrane elements with intact and compromised integrity, *Water Res.* 38 (2004) 3821–3832.